

Substitution of calcium with neodymium and dysprosium in hydroxyapatite structure

*E.I.Get'man, S.N.Loboda, T.V.Tkachenko,
A.V.Ignatov, T.F.Zabirko*

Donetsk National University, 24 Universitetskaya St.,
83055 Donetsk, Ukraine

Received May 20, 2004

Using X-ray phase analysis, the calcium substitution with Nd and Dy in hydroxyapatite $\text{Ca}_{10-x}\text{Ln}_x(\text{PO}_4)_6(\text{OH})_{2-x}\text{O}_x$ at 1100°C has been established to take place up to $x = 2.0$ and 1.4 , respectively. The IR spectroscopy has shown that along with the $\text{Ca}^{2+} + \text{OH}^- \rightarrow \text{Ln}^{3+} + \text{O}^{2-}$ substitution, the $2\text{OH}^- \rightarrow \text{O}^{2-} + \square$ one occurs. The structure refinement using Rietveld method has shown that Nd and Dy ions occupy mainly the Ca(2) positions. The $\text{Ca}^{2+} + \text{OH}^- \rightarrow \text{Ln}^{3+} + \text{O}^{2-}$ substitution has been established to strengthening of the Ca(2)–O(4) bond but weakens somewhat the Ca(2)–O(1,2,3) ones.

Методом рентгенофазового анализа установлено, что замещение кальция на Nd и Dy в гидроксиапатите $\text{Ca}_{10-x}\text{Ln}_x(\text{PO}_4)_6(\text{OH})_{2-x}\text{O}_x$ при температуре 1100°C происходит в области до $x = 2.0$ и 1.4 соответственно. Методом ИК спектроскопии показано, что наряду с замещением $\text{Ca}^{2+} + \text{OH}^- \rightarrow \text{Ln}^{3+} + \text{O}^{2-}$ имеет место и замещение $2\text{OH}^- \rightarrow \text{O}^{2-} + \square$. Уточнением структуры методом Ритвельда показано, что ионы неодима и диспрозия занимают преимущественно позиции Ca(2). Установлено, что замещение $\text{Ca}^{2+} + \text{OH}^- \rightarrow \text{Ln}^{3+} + \text{O}^{2-}$ приводит к упрочнению связи Ca(2)–O(4) и некоторому ослаблению связей Ca(2)–O(1,2,3).

Calcium hydroxyapatite $\text{Ca}_{10}(\text{PO}_4)_6(\text{OH})_2$ is the main inorganic component of the human bone tissue and finds its use as a bioactive material. The ability of apatites to isomorphic substitutions allows to use these materials in wastewater purification from heavy metal ions and as matrices for radioactive waste burial [1–3]. Solid solutions with apatite structure exhibit a catalytic activity in organic synthesis reactions [4, 5]. Apatites activated with RE ions have luminescence properties [6]. When calcium is substituted with Ln(+3) ions, the charge compensation is provided by inclusion of ions carrying lower positive charge, M(+1) and Si(+4), into the structure. For apatite single crystals, Ln uptake from the melt is weakened in the La–Nd–Sm–Dy sequence [7]. In the absence of foreign cations, calcium substitution with Ln(+3) is accompanied by the hydroxyl group transformation into oxide ion O^{2-} .

Synthetic apatites $\text{Ca}_8\text{Ln}_2(\text{PO}_4)_6\text{O}_2$ where Ln = La, Pr–Ho obtained by solid phase reactions at 1100°C [8] cannot be considered as homogeneous in all cases.

Of interest is the metal ion distribution in Ca(1) and Ca(2) positions [7–13] that defines the formation of discrete energy level system. To date, this problem cannot be solved a priori basing on the crystal-chemical properties of atoms substituting each other. Thus, the purpose of this work is to determine the substitution limits in the case of calcium substitution with Nd and Dy ions at the lowest temperature providing the apatite phase formation as well to study some features of its structure.

The samples of $\text{Ca}_{10-x}\text{Nd}_x(\text{PO}_4)_6(\text{OH})_{2-x}\text{O}_x$ (I) and $\text{Ca}_{10-x}\text{Dy}_x(\text{PO}_4)_6(\text{OH})_{2-x}\text{O}_x$ (II) were obtained using solid phase reactions, by successive calcination at 300 , 800 , and 1100°C at intermediate grinding. Calcium carbonate

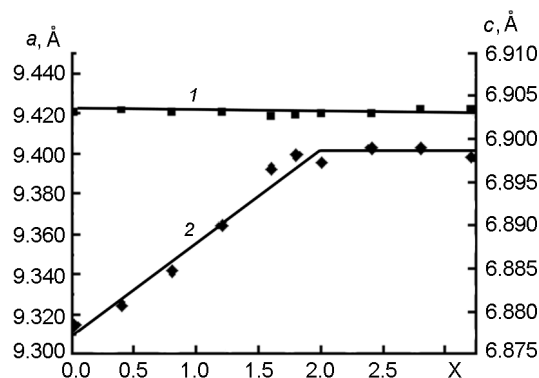


Fig. 1. Dependences of unit cell parameters a (1) and c (2) in $\text{Ca}_{10-x}\text{Nd}_x(\text{PO}_4)_6(\text{OH})_{2-x}\text{O}_x$ on the apatite composition.

and ammonium hydrophosphate (Special purity grade), neodymium and dysprosium oxides (No-CC and Di-2 grade, respectively) were used as initial materials. The high-temperature synthesis step was carried out for 20 h until the constant phase composition was obtained. The samples of system (I) belonging to solid solution region were calcined additionally in water vapor atmosphere at 900°C for 5 h. The samples were studied using X-ray phase analysis (XPA; URS-50im and DRON-2 instruments) with $\text{Cu K}\alpha$ radiation. The counter rotation speed was 1 deg/min in the phase analysis and 0.25 deg/min at the interplanar distance determination. The lattice parameters were calculated using 213 and 410 reflections of the hexagonal structure. Silicon was used as the internal standard. The crystal structures were refined by the Rietveld method [14]. To that end, X-ray powder diffraction data were collected in a regime: step 0.05 deg (2 θ); angle range $15.00 \leq 2\theta \leq 140^\circ$; scanning rate 10 s per step. The IR spectra were measured in the $4000\text{--}400\text{ cm}^{-1}$ for tablets (3 mg in 300 mg KBr) using a Perkin-Elmer Spectrum BX Fourier spectrophotometer.

According to the XPA data, the $\text{Ca}_{10-x}\text{Nd}_x(\text{PO}_4)_6(\text{OH})_{2-x}\text{O}_x$ system samples at $0 \leq x \leq 2$ calcined at 1100°C are single-phase ones having the apatite structure (space group P63/m). As the composition is varied, the reflection intensities change appreciably while the position thereof change only slightly. This is associated with close ionic radii values of Ca (1.12 Å) and Nd (1.109 Å) [15]. At $x > 2$, two additional phases with neodymium oxyphosphate Nd_3PO_7 and orthophosphate NdPO_4 (monoclinic symmetry) were established to be

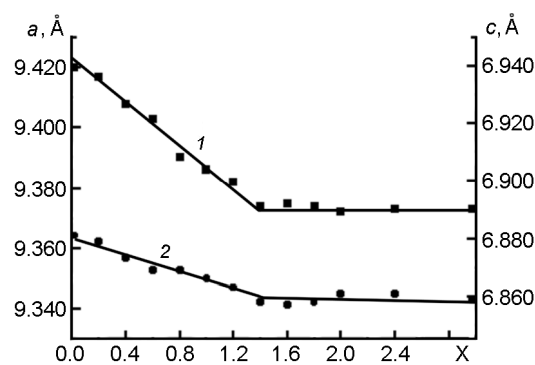


Fig. 2. Dependences of unit cell parameters a (1) and c (2) in $\text{Ca}_{10-x}\text{Dy}_x(\text{PO}_4)_6(\text{OH})_{2-x}\text{O}_x$ on the apatite composition.

formed along with the apatite phase. The dependence of c parameter on the Nd content (Fig. 1) in the homogeneity region is described by the straight line equation c (Å) = $6.877 + 0.011x$ (correlation coefficient 0.99) while the a parameter is essentially independent of Nd content. Basing on the lattice parameter dependence on Nd content and taking into account the sample phase composition, it can be concluded that the substitution limit in the scheme $\text{Ca}^{2+} + \text{OH}^- \rightarrow \text{Nd}^{3+} + \text{O}^{2-}$ coincides with the theoretically possible $x = 2$.

The phase composition of the $\text{Ca}_{10-x}\text{Dy}_x(\text{PO}_4)_6(\text{OH})_{2-x}\text{O}_x$ system (II) samples and the lattice parameter dependence on x (Fig. 2) indicate that the homogeneity region on the basis of apatite structure is limited by $x = 1.4$. At higher Dy content, phases with Dy_3PO_7 and monoclinic DyPO_4 structures are formed, too. The unit cell parameter dependences on Dy content within the range $0 \leq x \leq 1.4$ are described as a (Å) = $9.421 - 0.034x$ and c (Å) = $6.881 - 0.016x$ at correlation coefficient 0.99 in both cases. The lattice parameter diminishing as x increases agrees with the Dy^{3+} ion radius (1.027 Å).

The hydroxyl group presence in hydroxyapatites was determined from the IR absorption bands corresponding to stretching and librational modes of OH groups. The spectra of the (I) system samples measured after calcination at 1100°C are shown in Fig. 3. The absorption bands in $1090\text{--}960$ and $600\text{--}460\text{ cm}^{-1}$ are ascribed to PO_4^{3-} ion vibrations [16]. In the IR spectrum of calcium hydroxyapatite (system (I), $x = 0$), the presence of non-aqueous hydroxyl groups has been determined from 3572 and 632 cm^{-1} absorption bands corresponding to

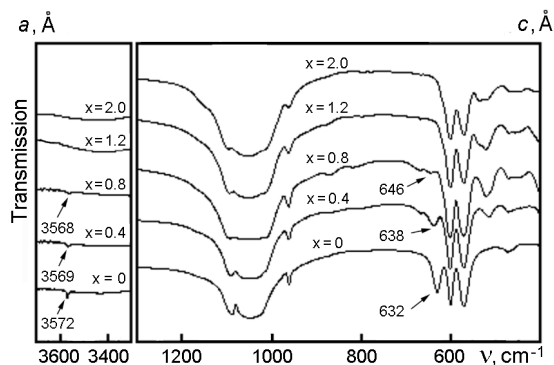


Fig. 3. Fragments of $\text{Ca}_{10-x}\text{Nd}_x(\text{PO}_4)_6(\text{OH})_{2-x}\text{O}_x$ absorption spectra.

to stretching and librational modes of OH. When calcium is substituted with neodymium, these bands decrease in intensity as x rises from 0 to 0.8; the bands are absent at higher x values. As neodymium content in solid solutions increases, the absorption bands associated with the stretching vibrations of OH groups are shifted towards lower frequencies while the frequencies ascribed to librational modes increase (Fig. 4a). These data are in agreement with the character of relative shifts of the stretching and torsion vibrations in the case of Ca substitution with Sr and Ba as well as of OH^- with F^- [17, 18]. A shift of the absorption bands associated with internal vibrations in phosphate groups has been found, it is the most pronounced for the middle band ν_3 (Fig. 4).

Calcium substitution with neodymium is accompanied also by appearance of several bands in the spectra ascribed to Nd–O bond vibrations [8–10]. In the $0.4 \leq x \leq 1.2$ range, the Nd–O vibrations are presented by a single band with wave number increasing from 516 to 522 cm^{-1} (Fig. 4a). Moreover, an additional band at 536 cm^{-1} appears in the spectra of samples where no OH vibrations are observed. Before, it has been reported [9, 10] that when Ln atoms occupy the Ca(2) site, the Ln–O vibration frequencies depend on the $\text{OH}^-/\text{O}^{2-}$ ratio in hexagonal channels of the structure. After the calcination of system (I) samples with x values from 0 to 1.2 in water vapor, a slight (2 to 3 cm^{-1}) decrease of Nd–O vibration frequency in the 516–522 cm^{-1} region is revealed accompanied by its intensity rise is observed while the $\nu = 536 \text{ cm}^{-1}$ band ($x = 1.2$) disappears.

The spectra of the system (II) samples where Ca is substituted with Dy are similar in character to those of Nd-substituted apa-

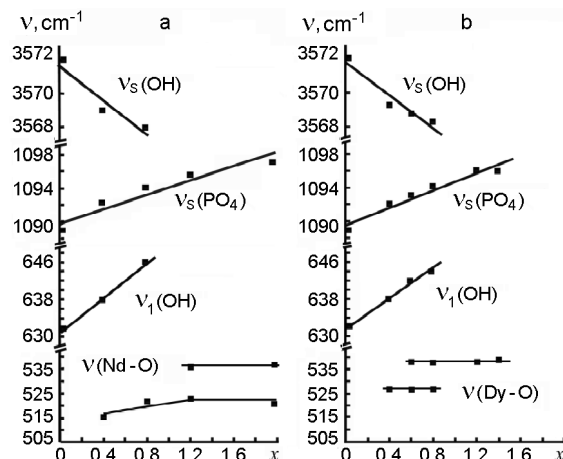


Fig. 4. Dependence of vibration frequencies in IR spectra on the composition of $\text{Ca}_{10-x}\text{Nd}_x(\text{PO}_4)_6(\text{OH})_{2-x}\text{O}_x$ (a) and $\text{Ca}_{10-x}\text{Dy}_x(\text{PO}_4)_6(\text{OH})_{2-x}\text{O}_x$ (b).

tites. The absorption bands related to OH vibrations are found at $x \leq 0.8$; as the dysprosium content increases, the OH stretching vibration frequencies decrease while the librational ones increase (Fig. 4b). Additional absorption bands at 527 and 538 cm^{-1} are also found and ascribed to the Dy–O bond vibrations; the first band intensity decreases and the second one increases as Dy content in apatites rises. A general feature of the IR spectra for the (I) and (II) system samples in the absence of hydroxyl group absorption bands in solid solutions where $x > 0.8$. This is due both to $\text{Ca}^{2+} + \text{OH}^- \rightarrow \text{Ln}^{3+} + \text{O}^{2-}$ substitution and to $\text{OH}^- \rightarrow \text{O}^{2-} + \square$ [19].

Thus, it follows from IR spectroscopy data that the change in OH group content in modified hydroxyapatite influences the position and intensity of bands according to Nd(Dy)–O bond, that agrees with the data on Ca substitution with La in hydroxyapatite [9]. Moreover, introduction of Nd^{3+} or Dy^{3+} into the hydroxyapatite structure results in shifted bands of stretching and librational modes of OH groups contained in the structure channels. Thus, basing on IR spectroscopy results, Nd^{3+} and Dy^{3+} ions can be supposed to substitute for Ca in the Ca(2) position, that is, in the $\text{Ca}(2)\text{O}_7$ polyhedra. This is in agreement with the structure refinement by Rietveld method. The calculated site occupancies (FULLPROF program) evidences that Ln(+3) ions are arranged predominantly in the Ca(2) position; Nd prefers the Ca(2) site in a much more pronounced fashion than Dy (Table 1). A

Table 1. Site occupancies and agreement factors

	Ca _{10-x} Dy _x (PO ₄) ₆ (OH) _{2-x} O _x			Ca _{10-x} Nd _x (PO ₄) ₆ (OH) _{2-x} O _x
	x = 0	x = 0.8	x = 1.4	x = 2.0
Ca(1) (4f)	4	3.868	3.868	3.932
Ln(1) (4f)	0	0.132	0.132	0.068
Ca(2) (6h)	6	5.334	4.734	4.068
Ln(2) (6h)	0	0.666	1.266	1.932
Ln(2)/Ln(1)	–	5.0	9.6	28.4
R _B , %	7.70	7.98	8.79	6.78
R _p , %	11.0	4.69	5.77	7.20
R _{wp} , %	14.6	5.97	7.41	9.46
χ ²	1.36	1.34	1.37	1.36

Table 2. Interatomic distances in Ca_{10-x}Ln_x(PO₄)₆(OH)_{2-x}O_x apatites

Distance, Å	x = 0 Dy	x = 0.8 Dy	x = 1.4 Dy	x = 2.0 Nd
Ca(1)–O(1) ×3	2.358(8)	2.373(9)	2.31(2)	2.37(1)
Ca(1)–O(2) ×3	2.460(8)	2.46(1)	2.49(2)	2.45(1)
Ca(1)–O(3) ×3	2.772(8)	2.765(8)	2.79(2)	2.779(9)
<Ca(1)–O>	2.530	2.53	2.53	2.53
Ca(2)–O(1)	2.69(1)	2.72(1)	2.78(2)	2.77(1)
Ca(2)–O(2)	2.36(1)	2.42(1)	2.50(3)	2.55(2)
Ca(2)–O(3) ×2	2.559(7)	2.557(7)	2.53(1)	2.583(9)
Ca(2)–O(3) ×2	2.292(6)	2.328(6)	2.36(1)	2.380(8)
<Ca(2)–O(1–3)>	2.46	2.49	2.51	2.54
Ca(2)–O(4)	2.404(5)	2.304(5)	2.218(7)	2.175(6)
<Ca(2)–O(1–4)>	2.453	2.463	2.462	2.488
P–O(1)	1.59(1)	1.56(1)	1.60(3)	1.57(2)
P–O(2)	1.53(1)	1.51(1)	1.46(3)	1.51(2)
P–O(3) ×2	1.577(6)	1.548(7)	1.52(1)	1.533(9)
<P–O>	1.57	1.54	1.53	1.54
Ca(2)–Ca(2)	4.084(6)	3.932(6)	3.84(1)	3.747(5)

similar trend is seen in apatites of different compositions [7, 9].

As calcium is substituted with Dy (as well as with Nd), the Ca(2)–O(4) distance is shortened substantially (by 0.19 and 0.22 Å, respectively; see Table 2). Here, O(4) denotes atoms situated in the structure channels. Shortened are also Ca(2)–Ca(2) distances between atoms situated at the vertices of calcium triangles. According to [8], this is due to increase in the binding energy caused by Ca²⁺ and OH[–] ions replacement by those (Ln³⁺, O^{2–}) having higher charges. The mean Ca(2)–O distance in seven-vertex Ca(2)O₇ polyhedra increases slightly (by 0.01 to 0.03 Å); but the mean distance between Ca(2) and six oxygen atoms related to PO₄ tetrahedrons increases more considerably (by 0.05 to 0.08 Å for limiting compo-

sitions). The increase of Ca(2)–O(1,2,3) distance in the case of Ca → La substitution [8] can be explained by a larger La size as compared to Ca. The Dy size is, however, much smaller than that of Ca. Therefore, the increased distance between Ca(2) and six oxygen anions seems to be associated with the increased binding energy of Ca(2)–O(4) bond. As a consequence, the Ca(2)–O(4) distance is shortened considerably while the other distances in seven-vertex units become somewhat longer. In this case, the Ca(2)–O(4) distance becomes the shortest in the Ca(2)O₇ unit.

On the other hand, the shift of Ln–O absorption bands in the IR spectra towards larger wave numbers due to the composition changes can be supposed to be associated, among other causes, with increased Ln–O

binding energy being a consequence of the shortened Ca(2)–O(4) distance. As to other interatomic distances, some "compression" of phosphate ions can be noted similar to that observed in [9] (the mean P–O distanced are shortened by 0.03–0.04 Å), the size of the Ca(1)O₉ polyhedra remaining essentially unchanged. The established regions of calcium substitution with neodymium and dysprosium in hydroxyapatite Ca_{10-x}Ln_x(PO₄)₆(OH)_{2-x}O_x at 1100°C are in correlation with the radii of the substituting ions. The introduction of Ln⁺³ ions into Ca(2) position is associated with the local compensation of O²⁻–Ln³⁺ charges resulting in a strengthening of Ca(2)–O(4) bond and some weakening of Ca(2)–O(1,2,3) ones.

References

1. J.C.Seaman, J.S.Arey, P.M.Bertsch, *J. Environ. Qual.*, **30**, 460 (2001).
2. P.Zhang, J.A.Ryan, *Environ. Sci. Technol.*, **33**, 625 (1999).
3. J.S.Arey, J.C.Seaman, P.M.Bertsch, *Environ. Sci. Technol.*, **33**, 337 (1998).
4. S.Sugiyama, K.Abe, T.Minami et al., *Applied Catalysis A: General*, **169**, 77 (1998).
5. K.Yamaguchi, K.Mori, T.Miguzaki et al., *J. Am. Chem. Soc.*, **122**, 7144 (2000).
6. G.Blasse, *J. Solid State Chem.*, **14**, 181 (1975).
7. M.E.Fleet, X.Liu, Y.Pan, *J. Solid State Chem.*, **149**, 391 (2000).
8. M.E.Escobar, E.J.Baran, *Monatsh. Chem.*, **113**, 43 (1982).
9. A.Serret, M.V.Cabanas, M.Vallet-Regi, *Chem. Mater.*, **12**, 3836 (2000).
10. A.Taitai, J.L.Lacout, *J. Phys. Chem. Solids*, **48**, 629 (1987).
11. P.E.Mackie, R.A.Young, *J. Appl. Cryst.*, **6**, 26 (1973).
12. V.S.Urusov, V.O.Khudolozhkin, *Geokhimia*, 1509 (1974).
13. L.W.Schroeder, M.Mathew, *J. Solid State Chem.*, **26**, 383 (1978).
14. J.Rodriguez-Carvajal, Program FullProf.2k (version 2.20-September 2002-LLB JRS) (unpublished).
15. R.D.Shannon, *Acta Cryst.*, **32A**, 751 (1976).
16. B.O.Fowler, *Inorg. Chem.*, **13**, 194 (1974).
17. B.O.Fowler, *Inorg. Chem.*, **13**, 207 (1974).
18. G.Knubovets, L.D.Kislovsky, in: *Crystal Chemistry of Minerals and Geology Problems*, ed. by A.G.Kossovsкая, Nauka, Moscow (1975), p.212 [in Russian].
19. J.C.Trombe, G.Montel, *Inorg. Nucl. Chem.*, **40**, 15 (1978).

Заміщення кальцію на неодим та диспрозій у структурі гідроксиапатиту

Є.І.Гетьман, С.М.Лобода, Т.В.Ткаченко,
О.В.Ігнатів, Т.Ф.Забірко

Методом рентгенофазового аналізу встановлено, що заміщення кальцію на Nd і Dy у гідроксиапатиті Ca_{10-x}Ln_x(PO₄)₆(OH)_{2-x}O_x при температурі 1100°C відбувається в області до x = 2,0 і 1,4 відповідно. Методом ІЧ спектроскопії показано, що поряд із заміщенням Ca²⁺ + OH⁻ → Ln³⁺ + O²⁻ має місце і заміщення 2OH⁻ → O²⁻ + □. Уточненням структури методом Рітвельда показано, що іони неодиму і диспрозію займають переважно позиції Ca(2). Встановлено, що заміщення Ca²⁺ + OH⁻ → Ln³⁺ + O²⁻ приводить до зміцнення зв'язку Ca(2)–O(4) і деякому ослабленню зв'язків Ca(1)–O(1,2,3).